討11 RAPID SOLIDIFICATION OF LEVITATION MELTED Ni-Sn ALLOY DROPLETS WITH HIGH UNDERCOOLING

Massachusetts Institute of Technology
The Castings Research Lab. Waseda Univ. Yuh Shiohara

Massachusetts Institute of Technology Merton C. Flemings
Yanzhong Wu
Thomas J. Piccone

INTRODUCTION

Undercooling ("supercooling") of metal alloys has been the subject of extensive study for over 30 years. Many of the early studies dealt with the homogeneous and heterogeneous nucleation of undercooled melts, beginning with the seminal work of Holloman and Turnbull [1]. Later studies also considered growth behavior and resulting structures of undercooled melts; notable examples being the work of the following individuals and their co-workers: Colligan [1], Flemings [2], Glicksman [3], Ohira [4], Shingu [5], Umeda [6], and Perepezko [7]. Work on both metallic and non-metallic systems has shown that the structures observed in bulk undercooled materials are determined to large extent by coarsening [3, 8].

Interest in solidification behavior of undercooled melts has been renewed in recent years, partly because of technical and scientific interest in rapid solidification processing. Undercooling plays a major role in determining the structures observed in many rapid solidification processes. In experiments reported in this paper, recalescence behavior of small (9 mm dia.) droplets is measured by high speed optical temperature sensing. The recalescence curves so obtained are used to glean information on the solidification mechanism of the undercooled metal alloys. A technique of levitation melting with glass encasement is used to obtain high undercoolings.

EXPERIMENTAL PROCEDURE

The experimental apparatus consists of a high frequency levitation melter, a two-color pyrometer, and a data storage and manipulation system. The levitation coil was constructed of 3.2 mm diameter copper tubing, covered with fiberglass tape and wound into a coil having primary and reverse turns. The experimental apparatus is shown schematically in Figure 1.

The metal sample was a nickel-tin binary alloy, which was the hypoeutectic Ni-25wt%Sn alloy. Samples were approximately spherical, made by pre-melting weighed amounts of high purity nickel wire (99.9999%) and tin shot (99.99999%) within a borosilicate glass medium similar to that used in the actual experiments. The liquidus temperature (1497 K) has been measured carefully using DTA (Differential Thermal Analysis) [9].

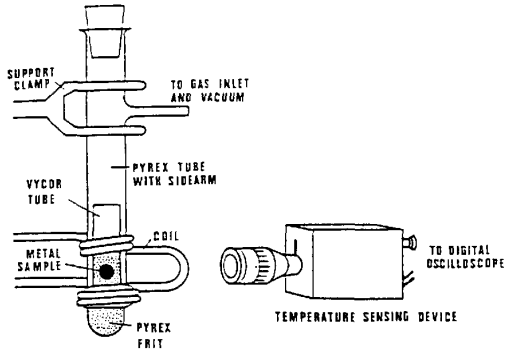

Figure 1. Schematic diagram of experimental apparatus.

The temperature measurement system consisted of two silicon photocells operating at near-infrared wavelength bands centered at 0.81 and 0.95 microns. The response time of the temperature measurement system was less than 20 microseconds.

Calibration of the temperature measurement system was performed by comparison of the two-color ratio with the temperature measured by a Pt/Pt-10%Rh thermocouple submerged within the sample. A linear relation between ratio and temperature was obtained, with a slope which did not vary with experimental conditions, and an intercept which varied slightly. The intercept was determined by calibrating the curve for each run using the eutectic "holds" on melting. Thermal data were filtered to reduce noise, using a linear low-pass filter for exponential smoothing.

In determining the recalescence and solidification times from thermal data, quantitative (although somewhat arbitrary) definitions were employed. Recalescence time was defined to be the time between the points of maximum curvature (positive and negative) in the temperature transient associated with recalescence. Solidification time was defined as the time between the first nucleation event and the inflection in the cooling curve after solidification.

RECALESCENCE AND COOLING CURVES

Thermal profiles for three typical samples with different initial undercoolings are shown in Figure 2. The thermal history of a sample at values of undercoolings up to about 260K consists of four features: (1) undercooling and nucleation; (2) a first recalescence event to the maximum recalescence temperature; (3) slow cooling to slightly below the eutectic temperature where a second nucleation event occurs: and (4) a thermal arrest, followed by continuous cooling. At values of undercooling higher than 260 K, only one recalescence was observed, followed by a thermal arrest.

A total of 50 experiments were conducted on the hypoeutectic alloy at undercoolings ranging from 22K

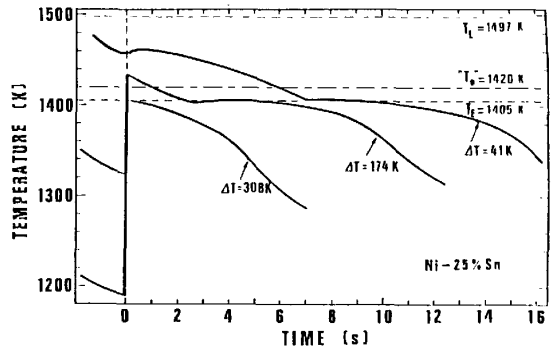

Figure 2. Thermal histories during solidification for three samples with different initial undercoolings (as labeled).

to 300K. Temperature recordings were made at sample rates ranging from a maximum of 20 microseconds per point (at which speed 40 milliseconds of data could be stored) to a minimum of 100 milliseconds per point (at which speed 20 seconds of data could be stored).

Solidification time for the samples as a function of undercooling is shown in Figure 3. The results for time between nucleation events and for recalescence time as functions of undercooling are also included. Solidification time and time between nucleation events both decreased linearly with increasing initial undercooling. The difference between solidification time and the time between nucleation events is the eutectic solidification time, which decreases only slightly with increasing undercooling. This may be taken as evidence that the weight fraction of eutectic is almost independent of initial undercooling for undercoolings up to about 260K.

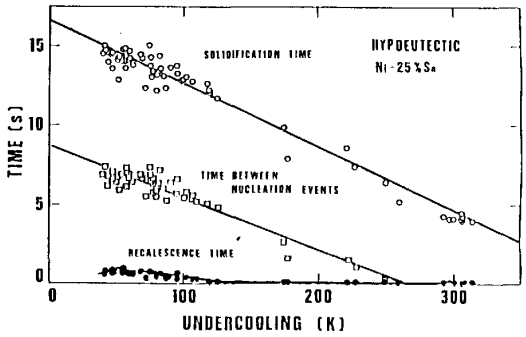

Figure 3. Plot of solidification time and time between two nucleation events as a function of initial undercooling. Recalescence time is also shown for comparison.

The recalescence time is very small compared to solidification time, and at high undercoolings it is negligible in comparison with total solidification time. The recalescence profiles for two typical samples with different initial undercoolings are shown in Figure 4. The arbitrarily defined start and end of recalescence are marked on these curves, and recalescence times, determined in this way for a large number of runs, are plotted in Figure 5 along with data from a separate study to be reported later on Ni-Sn samples of eutectic composition [9]. The data for both eutectic and hypoeutectic samples lie essentially on the same curve.

Experimental data for maximum recalescence temperature, T_R, when all undercooling is dissipated, are shown in Figure 6. This temperature decreases

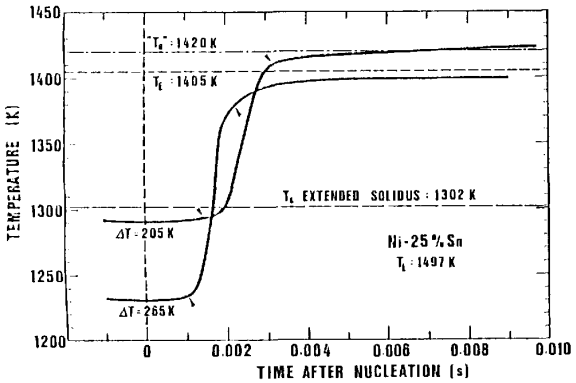

Figure 4. Thermal histories during recalescence for two typical samples with different initial undercoolings (as labeled).

to the eutectic temperature for samples undercooled over 250 K.

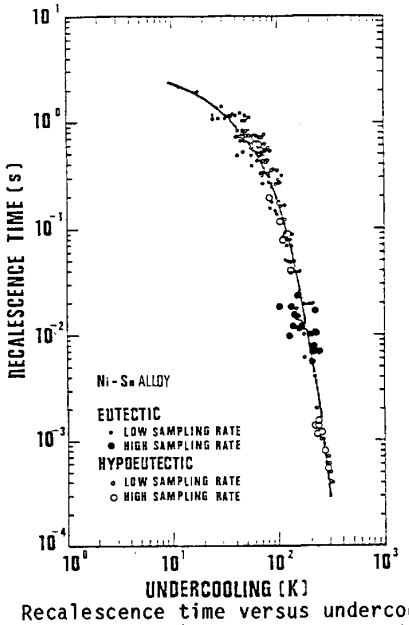

Figure 5. Recalescence time versus undercooling for Ni-25wt%Sn (hypoeutectic). Recalescence times for Ni-32.5wt%Sn (eutectic) are also shown for comparison [from 9].

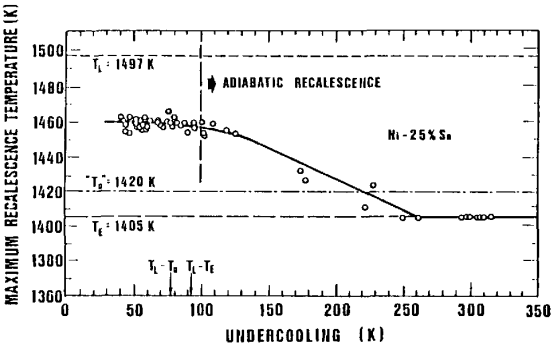

Figure 6. Maximum recalescence temperature versus undercooling.

CALCULATION OF ADIABATIC RECALESCENCE TEMPERATURE

A simple solute balance must describe the solid and liquid compositions and fractions at the maximum recalescence temperature, T_R where the fraction solid is f_s^R:

$$\bar{C}_s f_s^R + \bar{C}_L (1-f_s^R) = C_o \qquad (1)$$

where $\bar{C}_s$ is average composition of the solid, $\bar{C}_L$ is average composition of the liquid, and C_o is initial alloy composition. Assuming adiabatic conditions and specific heats of the solid and liquid are constant and equal, f_s^R is given by:

$$f_s^R = \frac{C_p}{\Delta H} (T_R - T_n) \qquad (2)$$

where C_p is specific heat (445 J/kgK), ΔH is heat of fusion (1.3×10^5 J/kg), and T_n is nucleation temperature.

Perhaps surprisingly, it will be seen that for high undercoolings the data for maximum recalescence temperature conform most closely to the assumption that solid and liquid compositions at the end of recalescence are uniform and at equilibrium, in which

case Equation 1 becomes the equilibrium lever rule [8]:

$$C_s f_s^R + C_L(1 - f_s^R) = C_o \quad (3)$$

where C_s and C_L are liquid and solid compositions as given by the equilibrium phase diagram at temperature T_R.

The curve drawn through the experimental data of Figure 6 for undercoolings greater than about 100K is a calculated curve based on (1) adiabatic recalescence, and (2) assumptions of equilibrium at the maximum recalescence temperature; i.e. on equations 2 and 3. Note the excellent agreement of experiment with theory, even for undercoolings greater than 260K where the maximum recalescence temperature is the eutectic temperature, implying nucleation of the second phase, β, during recalescence. Heat flow calculations discussed below also indicate that for the short recalescence times at undercoolings greater than 100K (i.e. recalescence times under 0.1 sec) recalescence should be adiabatic. For the longer recalescence times at lower undercoolings (0.1 to 2 sec) heat losses during recalescence appear sufficient to influence maximum recalescence temperature. Note this calculated curve corresponds closely to experimental results. A curve calculated as discussed below, also assuming "equilibrium" at the end of recalescence closely to experimental results in this regime.

Maximum recalescence temperatures calculated on any other basis than the "equilibrium" model above deviate very far from the experimental results. Examples would include calculations that assume significant solid supersaturation at the end of recalescence, without remelting during recalescence. Further it should be noted that calculations on other reasonable bases always result in a higher maximum recalescence temperature than that observed.

NON ADIABATIC RECALESCENCE TEMPERATURES

For recalescence times larger than about 0.1 seconds (undercoolings less than about 100 K) it seems likely that recalescence is no longer adiabatic. Heat transfer from the sample is by conduction to the glass and by radiation into the glass and through the glass to the surroundings. Consider a spherical metal sample embedded in a glass envelope sufficiently thick to be considered semi-infinite with respect to heat conduction. Metal and glass are cooled to the temperature, T_n, where nucleation occurs and recalescence of the metal begins. Heat flow then takes place from the metal to the glass by conduction and from the metal to the surroundings by radiation through the glass. If thermal gradients in the metal are small (i.e. recalescence is "Newtonian"), the heat balance is [10, 11]:

$$\rho_m V(C_p dT + \Delta H df_s) = [\sigma n^2 \varepsilon(T_e^4 - T^4) + h(T_b - T)]A dt \quad (4)$$

where V and A are the volume and surface area of the metal, respectively, ρ_m is the density of the metal ($\simeq 8.38 \times 10^3$ kg/m^3), f_s is the weight fraction of solid in the metal droplet, T is temperature, T_e is the temperature of the environment ($\simeq$ 300K), T_b is the glass temperature, t is time, and σ is the Stefan-Boltzmann constant (5.67×10^{-8} W/m^{2}K^4). n is the refractive index. ε and h are the emissivity for thermal radiation and conductive and convective heat transfer coefficient, respectively. Equations 4 and 3 with the phase diagram and experimentally measured recalescence times as a function of undercooling were used to calculate the non-adiabatic portion of the curve of Figure 6, assuming the emissivity, ε, is unity and the refractive index of the pyrex is 1.47. The agreement of calculation with experiment is excellent, although further experiments are necessary to determine if this simple heat transfer model is valid.

Total solidification time of the hypoeutectic alloy decreases linearly with increasing undercooling, Figure 4. This result is expected, at least for the higher undercooling because (1) recalescence time is negligible compared with total solidification time, (2) fraction liquid remaining to be solidified at the end of recalescence decreases approximately linearly with increasing undercooling, (3) rate of heat extraction after recalescence is approximately constant with time, and (4) cooling after recalescence is certainly Newtonian.

We anticipate that solidification after recalescence occurs as in usual dendritic solidification of castings and ingots so the "Scheil equation" adequately approximates solidification behavior. Central assumptions of this equation are no diffusion in the solid, complete diffusion in the liquid within interdendritic spaces and equilibrium at liquid-solid interfaces.

SOLIDIFICATION MECHANISM

The thermal data obtained in this work provide direct insight into the mechanism of solidification of the nickel-tin alloys during recalescence. We assume initial solidification is by dendritic growth within the bulk undercooled liquid, and that recalescence then continues as supersaturation of interdendritic liquid dissipates. Presumably the initial solid to form is the nickel-rich phase and in the early stages of recalescence we expect it to be relatively rich in tin, perhaps approaching C_o in composition.

The temperature rise during recalescence proceeds to the maximum temperature T_R where liquid and solid are at equilibrium and this requires that the composition of the solid dendrite decrease during the recalescence. This can be accomplished in the time allowed if melting occurs on a very fine scale within the dendrite arms.

At the higher undercoolings, the β phase (Ni_3Sn) is thermodynamically stable and could grow from a melt of composition C_o. This could occur at temperatures below 1350K, i.e. at undercoolings greater than about 150K. The β phase could also form at higher temperatures in liquid of composition greater than C_o. For example, liquid forming by remelting during recalescence would be expected to be richer in solute than C_o and this liquid, at all but the highest recalescence temperatures would be unstable with respect to β. The β phase that forms during recalescence is unstable above the eutectic temperature and must remelt. Clearly it does remelt (if it exists) both because of the fact that the "equilibrium" T_R is reached, and because on cooling back to the eutectic temperature a nucleation event is observed which must be β.

The arbitrary maximum recalescence temperature, T_R', is the point of maximum positive curvature on the recalescence curve. For undercoolings in excess of about 150K it is about 15K below the maximum recalescence temperature T_R. The shape of the curve in this final 15K of recalescence is strongly indicative of a ripening mechanism. This may be seen more clearly by plotting log $(T_R - T)$ versus log t for the recalescence as shown in Figure 7. Such plots, at least for undercoolings greater than about 150K typically show similar shapes with a sharp break occurring at about T_R' (i.e. at $T_R - T_R' \simeq 15$K). For the later stages of recalescence, the curves obtained are usually linear, as is the one shown.

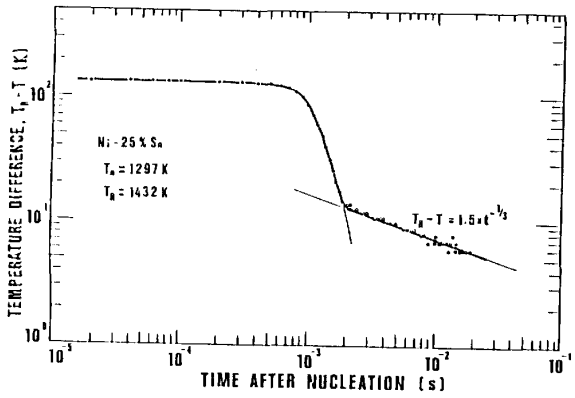

Figure 7. Temperature difference, T_R-T, versus time after nucleation, where T_R is the maximum recalescence temperature assumed to be 1432K.

This line has a slope of -1/3 as would be expected from coarsening theory. The experiments, however, do not provide unambiguous proof that the slope is always -1/3, because to do so requires knowing T_R to certainly less than one degree centigrade, and that is greater than the degree of certainty in these data.

Assuming growth at and above T_R' is totally controlled by coarsening, $(T_R - T_R') = 15$K and particles are spherical, the average particle size would be about .04 microns at T_R. They then coarsen significantly during the remainder of recalescence and subsequent cooling to the final solidification temperature.

The cooling curves after recalescence confirm two important aspects of the solidification model described above. The first is that the phase existing at the maximum recalescence temperature must be α since nucleation of β is observed on recooling to the eutectic temperature. The second is that the amount of eutectic which solidifies at the eutectic temperature is the amount expected if the solid present at the end of recalescence is at equilibrium.

In summary, the thermal data obtained in this work suggest a solidification model involving a series of presumably overlapping steps: (1) dendritic growth within the bulk undercooled melt, (2) continued recalescence as supersaturation of the interdendritic liquid dissipates, (3) fine scale remelting within the dendrites, thus permitting achievement of equilibrium solid composition toward the end of the short recalescence, (4) ripening of the fine structure that evolves in the later stages of recalescence, and (5) solidification of remaining liquid at the end of recalescence by extraction of heat to the surroundings.

We intend, in one or more papers to follow, to further elucidate this model through (1) experiments involving high speed photographic measurements of the recalescing droplet, (2) description of structures and solute distribution in samples produced, and (3) mathematical modeling of solidification during recalescence and comparison of this model with experimental results.

ACKNOWLEDGMENT

The authors express their deep gratitude to NASA for support of this work under Grant No. NSG 7645. They also acknowledge with thanks a number of student and others who have helped with various phases of the experimental work including Mr. R. Ewasko, Mr. D. Dellinger, and Mrs. M.W. Due. Discussions during the course of the work with Professor T.Z. Kattamis have been particularly helpful.

REFERENCES

1. G.L.F. Powell, and G.A. Colligan, Trans. AIME, 245, 1969, p.1913.
2. T.Z. Kattamis and M.C. Flemings, Met. Trans. 1, 1970, p.1449.
3. S.C. Huang and M.E. Glicksman, Acta Met., 29, 1981, p.717.
4. G. Ohira, Proc. U.S.-Japan Cooperative Science Program Semin. on "Solidification Processing", M.C. Flemings and G. Ohira (eds.), Dedham, MA 1983, p.1.
5. T. Ono, T. Takeo, T. Umeda, Y. Kimura, ibid., p.359.
6. K. Kobayashi, H.P. Shingu, Fourth International Conference on "Rapidly Quenched Metals", The Japan Institute of Metals, 1982, p.103.
7. J.H. Perepezko, "Rapid Solidification Processing, Principles and Technologies II", R. Mehrabian, B.H. Kear, and M. Cohen (eds.), Claitor Publishers, 1980, p.56.
8. M.C. Flemings, "Solidification Processing", McGraw-Hill, New York, 1974.
9. Y. Shiohara, T.J. Piccone, Y. Wu, and M.C. Flemings, To be published.
10. Y. Shiohara and M.C. Flemings, 'Modeling of Casting and Welding Processes II", Proc. 1983, Engineering Foundation Conf., Henniker, NH, TMS-AIME, 1984, p.165.
11. R. Gardon, J. Am. Ceramic Soc., 44, 1961, p.305.